Reduction Synthesis of Silver Nanoparticles Anchored on Silver Micro-Flakes and Electrical Resistivity of Isotropic Conductive Adhesives at Percolation Threshold

Sang-Soo Chee and Jong-Hyun Lee*

Department of Materials Science & Engineering, Seoul National University of Science and Technology,
Seoul 139-743, Korea

Reduction synthesis of silver in an ethanol solution without polyvinyl pyrrolidone was performed to anchor synthesized nanoparticles on micro-sized silver flake surfaces in order to enhance the electrical conductivity of isotropic conductive adhesives (ICAs). Although some shape-separated silver particles were formed, the synthesis of particles anchored on the flake surfaces was successful. The cured ICAs containing the silver flakes anchored with 1 wt. % nanoparticles indicated enhanced electrical conductivity due to their filling the gaps between noncontacting silver flakes at the beginning region of the percolation threshold. However, the anchored nanoparticles had a detrimental effect on the conductance when the content of anchored nanoparticles or flakes was higher.

Keywords: isotropic conductive adhesive (ICA), silver nanoparticle, reduction synthesis, electrical resistivity, percolation threshold

1. INTRODUCTION

Isotropic conductive adhesives (ICAs) have been used as interconnection materials for electronic applications for several decades, mainly because of their process-related convenience, despite their relatively low conductivity and high contact resistance in comparison with solders.[1,2] Hence, several studies have recently been performed with the aim of enhancing the electrical properties of ICAs. Improving the electrical properties mainly involves the addition of silver nanoparticles as conductive fillers or conductivity promoters in the fabrication of ICAs.[3-8]

According to descriptions in the literature, the electrical resistances of ICAs containing only nano-sized silver fillers are actually higher than those of conventional ICAs containing micro-sized silver flakes, and the resistances consistently increase with increasing particle content.[3,4] This can be attributed to contact losses among fillers due to the relatively reduced filler content and the increased numbers of series contacts involving nano-sized particles. Therefore, using silver nanoparticles as contact promoters in percolation linkages of micro-sized silver flakes is more favorable than using them as the complete structural material for percola-

tion linkages.[4,5,8] As an example, the addition of only ~1 wt. % silver nanoparticles was effective in reducing electrical resistance in the content of micro-sized silver flakes comprising the percolation threshold.[8]

On the other hand, the addition of silver nanoparticles was either negligible or detrimental to reducing the resistance in another case.[4,5] Hence, the usefulness of nanoparticles in improving electrical resistance in the filler content above the percolation threshold was not confirmed with certainty. Moreover, the influence of the minor addition of silver nanoparticles on the electrical resistance of micro-sized silver flakes at the percolation threshold has not been carefully studied.

In the conventional step of adding nano-sized silver fillers during the formulation of isotropic conductive adhesives, only a partial number of silver nanoparticles perch on the contact sites between micro-sized silver flakes. Most of the nanoparticles move freely in the binder material and reside in the spaces between the flakes during the subsequent high-rate shear mixing and curing steps. Moreover, the degree of dispersion of the silver nanoparticles is a very important factor in effectively enhancing the electrical properties of ICAs. To conclude, it would be better if the nanoparticles were anchored to the surfaces of the micro-sized flakes before the mixing, for them to be effective as contact promoters. The schematics depicting the estimated microstructures after cur-

(a) ICA containing
micro-sized Ag fillers

(b) ICA concurrently containing
micro- and nano-sized Ag fillers

(c) ICA containing micro-sized Ag
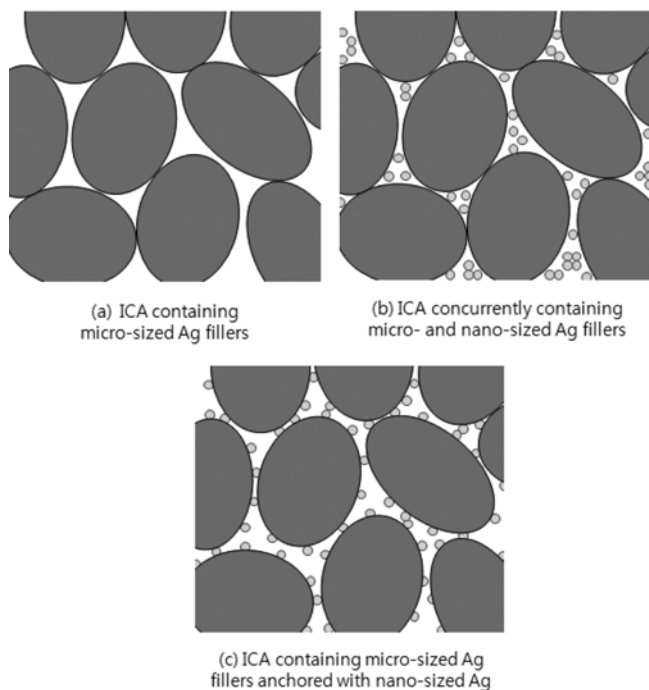fillers anchored with nano-sized Ag

Fig. 1. Schematics explaining the idea suggested in this study.

ing of the ICAs, fabricated with the methods mentioned above, are displayed as Fig. 1.

In this study, a technique of anchoring silver nanoparticles on micro-sized silver flake surfaces for preparing ICAs was attempted. The main purpose of the technique was to broaden the contact area between micro-sized silver flakes and make more conductive paths in the cured ICAs. Silver nanoparticles were synthesized on the flake surfaces via wet reduction synthesis, and then, the treated flakes were mixed with a snap-cure epoxy formation. The electrical resistances of the ICAs were scrutinized with respect to the content of nanoparticles at the percolation threshold.

2. EXPERIMENTAL

Micro-sized silver particles consisting of flake shapes with diameters of ~9.83 μm (FAG-80A) and ~4.36 μm (FAG-30A) were supplied by the Chang Sung Corporation. The two powders were mechanically mixed at a large-to-small weight ratio of 5.08, which gives the maximum packing density.

Silver nitrate ($AgNO_3$) (99.9%, Kojima Chemicals) and ethanol (99.9%, Duksan Pure Chemicals) were purchased for the synthesis of silver nanoparticles. For the synthesis of silver nanoparticles on the silver flake surfaces, the 2 g bimodal silver flakes were added into the 10 m*l* ethanol solution containing 0.085 g silver nitrate. The solution was indirectly heated to 60°C using a water bath and maintained for 210 min. The solution was continuously stirred with a mag-

netic bar during the synthesis procedure.

After the synthesis, the solution containing micro- and nano-sized particles was dried at room temperature using a vacuum chamber. The surfaces of the dried particles were then examined using a scanning electron microscope (SEM).

The silver flakes anchored with silver nanoparticles were mixed with an in-house epoxy formulation having snap-cure properties using a homogenizer as a function of filler content. Prior to this, the formulation was prepared by mixing an epoxy resin (EPON 862, Hexion Specialty Chemicals) with other ingredients, such as a hardener (hexahydro-4-methylphthalic anhydride, Sigma-Aldrich). The fabrication procedure for the epoxy formulation was similar to that shown in another article.[9] The paste was plastered on a slide glass and cured at 140°C for 60 s. The cured ICA was ground to a thickness of ~150 μm before the electrical resistance was measured. The resistance of the ICAs was measured using a multimeter (Keithley 2400, Keithley Instrument) with a four-point probe. At least five samples were prepared, and five points were measured for each specimen.

3. RESULTS AND DISCUSSION

3.1 Morphologies of silver nanoparticles synthesized without PVP

A reduction synthesis of silver using an ethanol vehicle has been reported in a previous article.[8,10-12] The reduction reaction can be expressed as follows:

$$C_2H_5OH \rightarrow CH_3-CH: +H_2O$$

$$CH_3-CH: +2Ag^+ +H_2O \rightarrow 2Ag +3H^+ +CH_3-CO^-$$
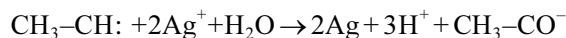
Chen *et al.* used polyvinyl pyrrolidone (PVP) as a capping agent in the ethanol-based reduction synthesis.[8,10] In this case, a complex compound containing silver ions and PVP is easily reduced at the early stage. Thus, the nucleation rate increases and a higher number of nuclei are formed, owing to the presence of PVP. In addition, the presence of PVP decreases the mean size of the particles collected because PVP plays a role in preventing silver nanoparticles from coagulating, by covering their surfaces.[13] However, the PVP covering layer has a big drawback, in terms of electrical conduction by the linkage between nanoparticles, because PVP is an electrically insulating material. Hence, the residual PVP content should be controlled,[14] or the silver nanoparticles synthesized in this manner should be repeatedly washed with acetone/water.[5,15]

In this study, the reduction synthesis of silver nanoparticles in the absence of PVP was attempted in order to prepare additive conducting fillers in ICAs. A prolonged reaction time of 210 min was permitted for the completion of the synthesis. As a result, the synthesis was successful, as observed
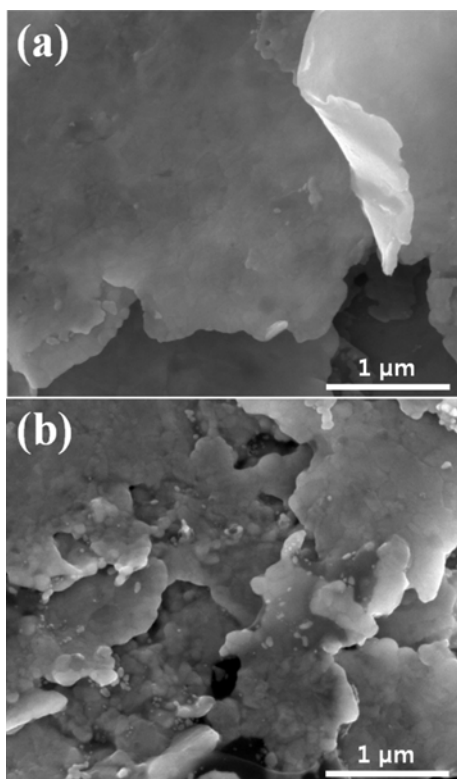
Fig. 2. SEM micrographs indicating morphologies of silver flakes (a) in a raw state and (b) after the synthesis of silver nanoparticles.

Fig. 3. SEM micrographs indicating the homogeneous nucleation and growth of silver and coagulation among nanoparticles during the synthesis without PVP.

in Figs. 2 - 4. Figure 2(b) shows the morphologies of silver nanoparticles synthesized on the micro-sized silver flakes without PVP. The amount of reduced silver was ~4% of the initial silver flake weight. From the microstructural comparison in Fig. 2, it was evident that most of the silver nanoparticles were attached to the surfaces of the silver flakes. More specifically, the silver nanoparticles were preferentially formed on the edges of the flakes, not on the smooth surfaces. Because the activation energy barrier of heterogeneous nucleation is smaller than that of homogeneous nucleation,[16] heterogeneous nucleation may become more feasible. Moreover, edge surfaces are considered as preferential sites for atom attachment because the surface energy remains unchained. Silver does not corrode in ethanol, therefore the uniformly sized, extremely small protuberant morphologies observed in the flat surfaces of the flakes, as shown in Fig. 2(b), also indicated synthesis behavior at the nano-size level. Meanwhile, the rough-shaped structures observed on the edges of the flakes displayed that the structures are agglomerates of nanoparticles. The absence of capping on nanoparticle surfaces from the synthesis without PVP may induce the agglomeration.

Some individual elongated spheres or irregular shapes are also observed after the synthesis, as shown in Fig. 3. Coagulation among disjoined small particles was estimated to
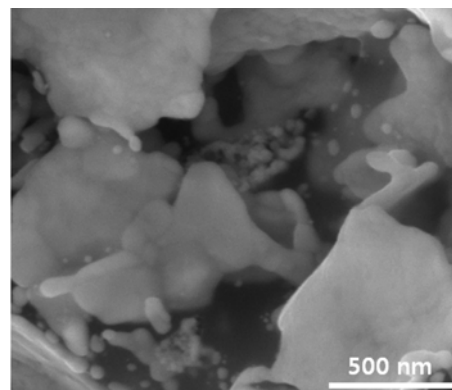
result in the formation of larger disjoined particles that were irregular in shape and size. Hence, the microstructural features resulting from the homogeneous nucleation and coagulation of silver nanoparticles during the reduction synthesis are simultaneously shown in Fig. 3. The shapes of the perfectly disjoined particles, thought to be formed through homogeneous nucleation and coagulation, were observed to be very similar to the rough-shaped nodule structures in the flake edges. The result strongly confirmed that particles up to several hundred nanometers in size were formed from the coagulation of primary particles and could attach to flake surfaces. In conclusion, the rough-shaped nodule structures attached to flake surfaces may be formed in two possible ways. On the one hand, nanoparticles, heterogeneously nucleated and grown through the reduction of silver, form directly on the silver flakes. On the other hand, they may eventually attach to the flakes, while some homogeneously nucleated and grown particles cannot settle initially on the flakes.

Figure 4 presents SEM images revealing the surface morphology changes in the silver flakes with respect to the amount of synthesized silver nanoparticles. The figures show that the protuberant morphologies in the silver flake surfaces rapidly increased along with an increasing amount of synthesized silver. Further, the sizes of the protuberant morphologies suddenly grew to a micro scale with an increase in the quantity of synthesized silver. As shown in Fig. 4(a), the initial nano-sized nodules have a large surface area and many edge surfaces. Thus, the initial nodules would be preferential sites for follow-up heterogeneous nucleation. Nevertheless, it is still difficult to explain the violent enhancement of the heterogeneous nucleation and growth on smooth surfaces with an increase in synthesized silver, which created big irregular skins. The most plausible mechanism explaining the violent formation of the irregular skins is likely to be the attachment behavior of the agglomerates
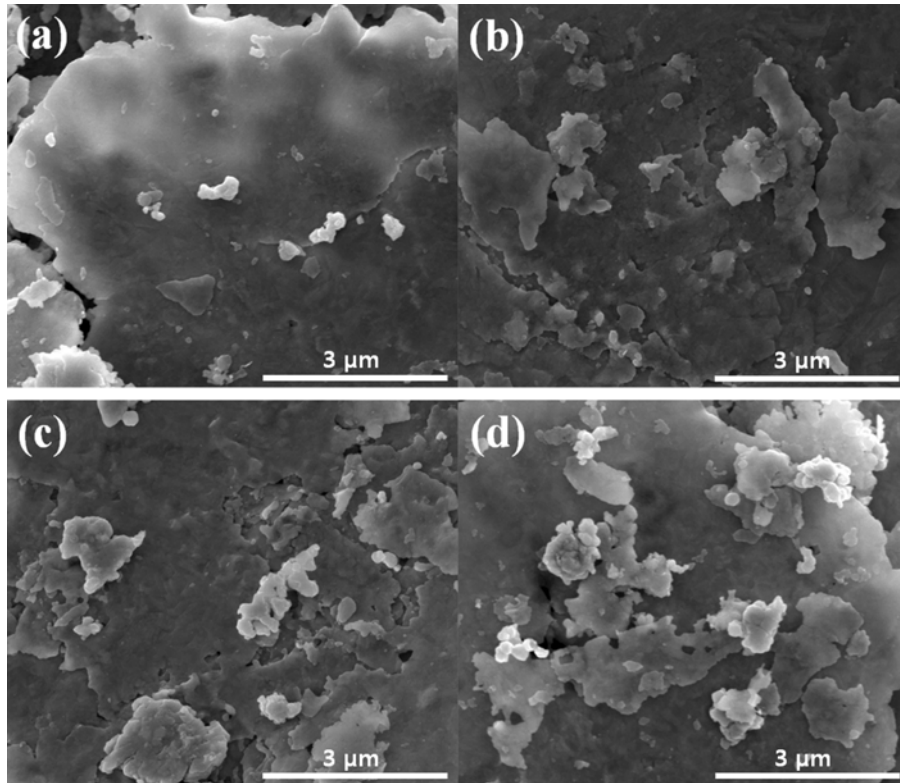
Fig. 4. Surface morphologies of silver flakes with respect to the amount of synthesized silver: (a) 1 wt. %, (b) 2 wt. %, (c) 3 wt. %, and (d) 4 wt. % of initial silver flake weight.

consisting of the particles synthesized from homogeneous nucleation and growth. The immethodical distribution of the skins may also be evidence for the attachment behavior of coagulated particles.

3.2 Electrical properties of cured ICAs

The electrical resistances of ICAs cured with only micro-sized or mixed-sized silver are simultaneously plotted in Fig. 5 as a function of the silver flake volume fraction. The electrical resistances of ICAs with mixed-sized silver were measured only at the percolation threshold. In the ICA containing only micro-sized silver flakes, the percolation threshold range was measured to be around 10.9 - 14.3 vol. %, resulting in a rapid decrease of resistivity with an increase in flake content. The resistance decreased to 1.18×10^{-3} $\Omega \cdot$cm for a silver flake content of 20.6 vol. %.

When silver nanoparticles corresponding to 1% of the silver flake weight were synthesized on 12 vol. % silver flakes, the resistance was observed to decrease dramatically. However, this was the only improved result obtained in our study. In the presence of 1 wt. % nanoparticles, the resistance tended to increase rapidly with an increasing volume fraction of silver flakes, to 14.3%. The anchored nanoparticles may be very effective in making contact points between flakes at the beginning region of the percolation threshold
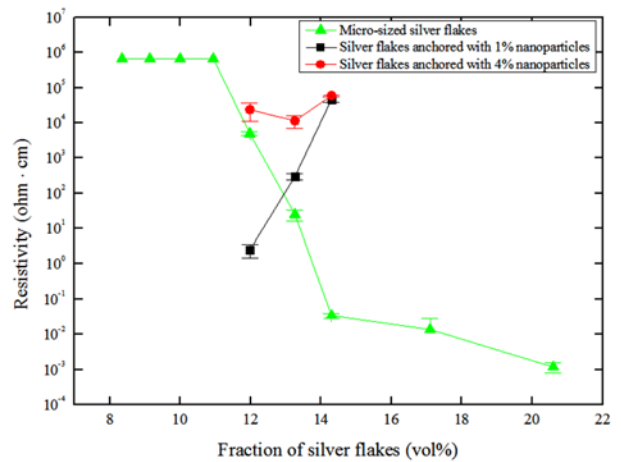

Fig. 5. Average electrical resistivity of cured ICAs measured as a function of the silver flake volume fraction and the quantity of silver nanoparticles synthesized.

because more conductive paths can be formed by filling the gaps between noncontacting silver flakes with slightly more filler content. However, the anchored nanoparticles at the end region of the percolation threshold, which assures sufficient contact points, are likely to cause an increase in the number of contact points in series, resulting in an overall

resistance increase. Considering an electrical conduction path in the ICAs containing only flakes, there would be just one contact resistance per unit linkage between the flakes. Meanwhile, the contact resistance per unit linkage in another structure consisting of flakes and nanoparticles can increase to at least two. Even though contact resistance in the interface between an anchored nanoparticle and a flake may be lower than that in the interface between flakes formed while making the composite structure, consisting of flakes and resin, the anchored nanoparticle/flake interface is still detrimental because it produces additional contact resistance. Consequently, the increase in contact points contributes a more dominant effect on electrical resistivity than the enhancement of the contact area from the middle range of the percolation threshold. Because the contacts between the flakes increased spontaneously with increasing flake content, the anchored nanoparticles demonstrated a detrimental effect to electrical conduction at the end region of the percolation threshold.

In the case with 4 wt. % nanoparticles, all ICAs containing flakes of around 12.0 - 14.3 vol. % showed higher resistance compared to those comprising only flakes. As clearly revealed from the image of Fig. 4(d), the greater the increase in silver content, the more the silver skins, formed by the reduction, were characterized as a multilayer structure. Hence, the total resistance would be multiplied as a result of having increased the series contact in the multilayer skins structure. Consequently, the thick silver layers anchored on the flakes by the synthesis of excessive amounts also manifested a detrimental effect to electrical conduction at the per-

colation threshold.

Figure 6 shows the microstructures observed after curing the ICAs containing 12 vol. % silver flakes anchored with silver nanoparticles, indicating suggested causes for interpreting the results of Fig. 5. In the case with 1 wt. % nanoparticles, the anchored nanoparticles generally formed a single layer and effectively filled the gaps between the noncontacting silver flakes to make more conductive paths. In the presence of 4 wt. % nanoparticles, however, the anchored nanoparticles were observed to be a multilayer structure, forming series contacts in the gaps between the untouched silver.

4. CONCLUSIONS

The reduction synthesis of silver in an ethanol solution containing micro-sized silver flakes was conducted to anchor synthesized nanoparticles on the flake surfaces and decrease the electrical resistance of ICAs. The number of particles anchored on the flake surfaces increased suddenly as the amount of reduced silver increased, although some shape-separated particles were formed due to homogeneous nucleation. This was probably due to the attaching and agglomeration behavior of the individual nanoparticles under stirring conditions, indicating successful synthesis without PVP. The cured ICAs containing 1 wt. % nanoparticles, which were anchored on the silver flakes, indicated enhanced electrical conductivity by reinforcing the deficient contact points between flakes in the beginning region of the percolation threshold. When the content of anchored nanoparticles or flakes was higher, the anchored nanoparticles had a detrimental effect on the conductance.

REFERENCES

1 J.-S. Lee, J.-K. Kim, M.-S. Kim, and J.-H. Lee, *Korean J. Met. Mater.* **47**, 447 (2009).
2. D.-H. Kim, S. Yoo, C.-W. Lee, and T.-Y. Lee, *J. Microelectron. Packag. Soc.* **17**, 55 (2010).
3. L. Ye, Z. Lai, J. Liu, and A. Thölén, *IEEE Trans. Electron. Pack. Manuf.* **22**, 299 (1999).
4. L. Fan, B. Su, J. Qu, and C. P. Wong, *Proc. 9th Int. Sympo. on Adv. Packag. Mater.: Processes, Prop. & Interface*, p. 193, IEEE, Atlanta, US (2004).
5. H.-H. Lee, K.-S. Chou, and Z.-W Shih, *Int. J. Adhes. Adhes.* **25**, 437 (2005).
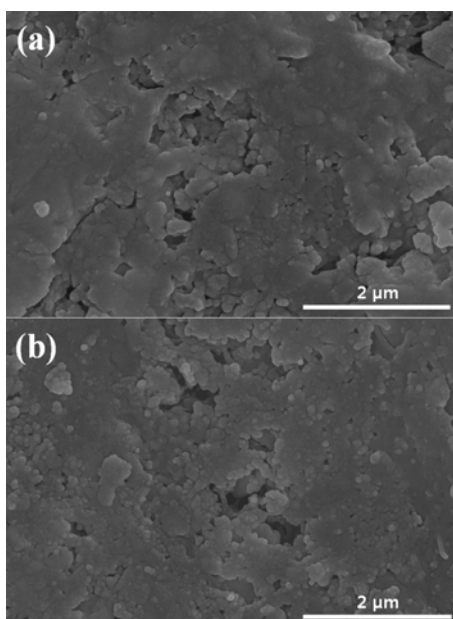6. X. Wang and Z. Zhang, *Proc. 6th Int. Conf. on Electron. Packag. Technol.*, p. 226, Harbin Institute of Technology,

Fig. 6. Microstructures observed after curing the ICAs containing 12 vol. % silver flakes anchored with (a) 1 wt. % (per weight of silver flakes) or (b) 4 wt. % silver nanoparticles.

Shenzhen, China (2005).

7. H. Jiang, K. Moon, J. Lu, and C. P. Wong, *J. Electron. Mater.* **34**, 1432 (2005).

8. D. Chen, X. Qiao, X. Qiu, and J. Chen, *J. Mater. Sci.* **44**, 1076 (2009).

9. J.-H. Kim, J.-K. Kim, C.-Y. Hyun, and J.-H. Lee, *J. Microelectron. Packag. Soc.* **17**, 41 (2010).

10. H. Chen, Y. Liu, and G. Zhao, *Electron. Mater. Lett.* **7**, 151 (2011).

11. S. Horiuchi, T. Fujita, T. Hayakawa, and Y. Nakao, *Langmuir* **19**, 2963 (2003).

12. J. Yang, T. C. Deivaraj, H.-P. Too, and J. Y. Lee, *Langmuir* **20**, 4241 (2004).

13. Z. Zhang, B. Zhao, and L. Hu, *J. Solid State Chem.* **121**, 105 (1996).

14. H.-H. Lee, K.-S. Chou, and K.-C. Huang, *Nanotechnology* **16**, 2436 (2005).

15. S. L.-C. Hsu and R.-T. Wu, *Mater. Lett.* **61**, 3719 (2007).

16. D. A. Porter and K. E. Easterling, *Phase Transformations in Metals and Alloys*, 2nd ed., p. 192, Chapman & Hall, London, UK (1992).